

Heavy quark bound states above T_c

W.M. Alberico, A. Beraudo, A. De Pace and A. Molinari

Dipartimento di Fisica Teorica dell'Università di Torino and

Istituto Nazionale di Fisica Nucleare, Sezione di Torino,

via P.Giuria 1, I-10125 Torino, Italy

(Dated: July 7, 2005)

Abstract

A comprehensive parameterization of the colour singlet heavy quark free energy above T_c is given, using the lattice data in quenched ($N_f = 0$) and unquenched ($N_f = 2$ and $N_f = 3$) QCD. The corresponding (temperature dependent) potentials thus obtained are then inserted into the Schrödinger equation for the charmonium and the bottomonium in the deconfined phase of QCD. The solution of the equation provides an estimate of the melting temperature and of the radii for the different $c\bar{c}$ and $b\bar{b}$ bound states.

PACS numbers: 10.10.Wx, 12.38.Gc, 12.38.Mh, 12.39.Pn, 14.40.Lb, 14.40.Nd, 25.75.Nq

I. INTRODUCTION

The anomalous suppression of the J/ψ production in heavy ion collisions, which has been experimentally observed [1, 2] in the depletion of the dilepton multiplicity in the region of invariant mass corresponding to the J/ψ meson, was proposed long time ago as a possibly unambiguous signal of the onset of deconfinement [3]. Indeed in Ref. [3] it is argued that charmonium states can only be produced in the first instants after the nucleus-nucleus collision, before the formation of a thermalized QGP. Then, in their path through the deconfined medium, the original $c\bar{c}$ bound states tend to melt, since the binding (colour) Coulomb potential is screened by the large number of colour charges. This, in turn, produces an anomalous (with respect to normal nuclear absorption) drop in the J/ψ yields.

In this picture it is implicitly assumed that, once the charmonium dissociates, the heavy quarks hadronize by combining with light quarks only (recombination leading to a secondary J/ψ production is neglected). This assumption is certainly justified at the SPS conditions, due to the very small number of $c\bar{c}$ pairs produced per collision ($N_{c\bar{c}} \sim 0.2$ in a central collision), but at RHIC ($N_{c\bar{c}} \sim 10$) and LHC ($N_{c\bar{c}} \sim 200$) energies it is no longer warranted [4].

Moreover in a hadronic collisions only about 60% of the observed J/ψ 's are directly produced, the remaining stemming from the decays of excited charmonium states (notably the χ_c and the ψ'). Since each $c\bar{c}$ bound state dissociates at a different temperature, a model of *sequential suppression* was developed, with the aim of reproducing the J/ψ suppression pattern as a function of the energy density reached in the heavy ion collision (the highest temperatures and energy densities being reached in the most central collisions) [5, 6, 7, 8, 9]. SPS experimental data for Pb-Pb collisions at different centralities seem indeed to support the dissociation pattern predicted by this model [1, 2].

Alternative mechanisms for the J/ψ production, like the Statistical Coalescence Model (SCM), have also been proposed [10]. In the SCM one assumes again that all the $c\bar{c}$ pairs are produced in hard processes at the initial stage of the collision. Any heavy quark bound state, if present, is assumed to melt in the QGP phase and the number of $c\bar{c}$ pairs in the fireball is considered fixed. At the chemical freeze-out open and hidden charmed hadrons

are then produced with multiplicity *ratios*¹ fixed by their masses, according to the laws of statistical mechanics. Hence, in such a scheme, the measured J/ψ multiplicity is not related to the presence of charmonium bound states in the plasma phase, but to the statistical hadronization of the initially produced $c(\bar{c})$ (anti-)quarks. This may lead, at LHC energies, to a completely different picture characterized by an enhanced charmonium production even if all the $c\bar{c}$ bound states dissociate during the plasma phase.

In any case the hypothesis that all the primary produced J/ψ 's melt during the QGP lifetime is hardly realized at SPS conditions. Hence models have been developed [11, 12] attempting to account both for the initial state production, eventually subject to in-medium dissociation, and for the thermal production at the hadronization.

Concerning the heavy quarkonia in the QGP phase, recent lattice data [13, 14, 15] in quenched approximation (hence neglecting effects arising from virtual processes involving dynamical fermions), which display narrow peaks for the charmonium spectral functions in the pseudoscalar and vector channels (even up to $T \sim 2T_c$), seem to point to the existence of heavy quark bound states up to temperatures above T_c ². Clearly these results, if confirmed, would entail striking experimental consequences.

Actually, the meson spectral functions cannot be measured directly on the lattice. From the numerical simulations one gets the current-current correlation function along the (imaginary) temporal direction on a finite number of points. Such a correlator corresponds to the convolution of the meson spectral function with a thermal kernel. The spectral function can then be obtained only indirectly. With this aim in Refs. [13, 14, 15] a procedure called Maximum Entropy Method (MEM) has been adopted. Clearly, an independent check of the results obtained with MEM appears desirable. This indeed is our scope in the present paper.

For this purpose, we first extract from lattice data a heavy quark potential accounting for thermal effects and then we solve the Schrödinger equation for the charmonium (and bottomonium). As shown in Refs. [16, 17, 18, 19, 20], from the Polyakov loop correlation function it is possible to extract the free energy (in the different color channels) of a heavy quark-antiquark pair placed at a distance r in a thermal bath of gluons and light dynamical

¹ Due to the low rate of inelastic reactions full chemical equilibrium cannot be reached by charmed hadrons: their total multiplicity measured at SPS stays well above the thermal value.

² Actually, in Ref. [14] the analysis has been done for $s\bar{s}$ mesons.

fermions. Once a good parameterization of the color singlet free energy is obtained, the entropy and internal energy contributions can be disentangled. Since the quarks acting as static sources of the color field are considered infinitely heavy, the internal energy coincides with the potential. The latter is then inserted into the Schrödinger equation, from which the binding energy of the different stable states — if there are any — and their evolution with the temperature are obtained.

Indeed a clear distinction between the $Q\bar{Q}$ free and potential energies is necessary in order to get a reliable estimate of the quarkonium dissociation temperature T_d in the different spin-parity channels.

In Refs. [6, 7, 21, 22], where the colour singlet *free energy* was directly inserted into the Schrödinger equation, the dissociation temperatures $T_d = 1.10T_c$ [7] and $T_d = 0.99T_c$ [21] were found for the J/ψ , all the other charmonium states melting well below T_c .

On the other hand, in Ref. [23], where a parameterization of the lattice color singlet *potential* (in the quenched approximation) was used, the temperature T_d for the *spontaneous dissociation* of the J/ψ was estimated to occur at about $2T_c$, a value even larger than the one obtained from the spectral analysis performed in Refs. [13, 14, 15]. Also results for different charmonium and bottomonium states have been reported in Ref. [23]. The case $N_f = 2$ was addressed in Ref. [24], where the J/ψ meson was found to be bound till $T \sim 2.7T_c$.

Actually, even if the potential supports the existence of bound states, other physical processes may lead to the dissociation of the quarkonium. First, if the $Q\bar{Q}$ binding energy is lower than the temperature — and assuming that the quarkonia have reached the thermal equilibrium with the plasma — a certain fraction of their total number will be thermally excited to resonant states according to a Bose-Einstein distribution: such a process is referred to as *thermal dissociation* [21, 23]. Furthermore, the collisions with the gluons and the light quarks of the plasma may lead to the *collisional dissociation* of the quarkonium. In this connection, the reaction $g + J/\psi \rightarrow c + \bar{c}$ was studied in detail in Ref. [23]. Hence, in spite of the presence of a bound state solution of the Schrödinger equation till $T \sim 2T_c$, the J/ψ turned out to be really stable only up to temperatures lower than $2t_c$ [23]. Clearly the two processes above mentioned are not encoded in the Polyakov loop correlation function, where the heavy quarks act as unthermalized static sources of the color field, and have to be accounted for *a posteriori*.

Of course, if the process $g + J/\psi \rightarrow c + \bar{c}$ can lead to the dissociation of the charmonium,

the same reaction can also occur in the opposite direction. Hence a consistent calculation of J/ψ multiplicity implies the solution of a kinetic rate equation integrated over the lifetime of the QGP phase in which both processes (dissociation and recombination) enter [23, 25]. To carry out this detailed balance calculation the knowledge of the J/ψ binding energy and wave function in the thermal bath turns out to be an important input. This is of relevance because, as mentioned above, the usual assumption in considering the J/ψ suppression as a signature of deconfinement is that its production can occur only in the very initial stage of the collision. Really, if at SPS the role played by recombination is numerically negligible, this is no longer true at RHIC as pointed out in Ref. [25].

In any case in this paper we limit ourselves to check the existence of bound state solutions of the Schrödinger equation. A quantitative study of the dissociation and recombination processes is left for future work.

Here we take advantage of all the available lattice data, obtained not only in quenched QCD ($N_f = 0$), but also including two and, more recently, three light flavors. We are then in a position to study also the flavor dependence of the dissociation process, a perspective not yet achieved by the parallel studies of the spectral functions, which are, as already mentioned, only available in quenched QCD.

The present paper is organized as follows. In Sec. II we present a parameterization of the color singlet free energy lattice data for the cases $N_f = 0$ [17], $N_f = 2$ [20] and $N_f = 3$ [26], from which the heavy quark potential is obtained. In Sec. III we solve numerically the associated Schrödinger equation at different temperatures for the charmonium and bottomonium states, thus determining their dissociation temperature. Finally, in Sec. IV we present our conclusions.

II. PARAMETERIZATION OF THE LATTICE DATA

In this section we provide a unified parameterization of the lattice data for the *color singlet* $Q\bar{Q}$ free energy F_1 in the case of quenched [17], 2-flavor [20] and 3-flavor [26] QCD. The lattice findings are shown (in dimensionless units) in Fig. 1.

For what concerns the critical temperature we assume the values $T_c = 270$ MeV ($N_f = 0$), $T_c = 202$ MeV ($N_f = 2$) and $T_c = 193$ MeV ($N_f = 3$) given in Ref. [20].

The free energy on the lattice is defined up to an additive normalization constant, which

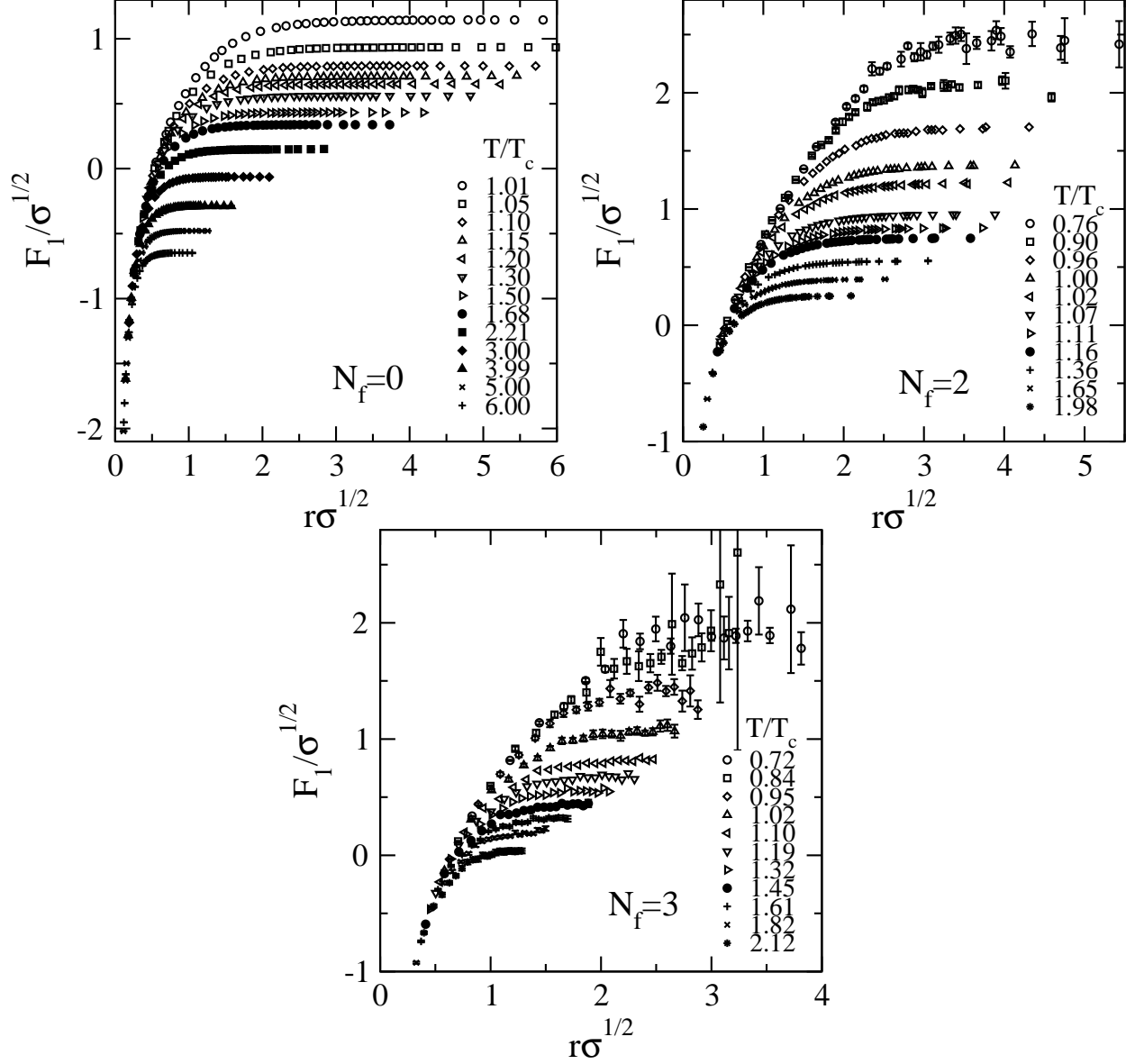


FIG. 1: A sample of the available data for $F_1(r, T)/\sqrt{\sigma}$ at different values of T/T_c as a function of the separation $r\sqrt{\sigma}$ of the $Q\bar{Q}$ sources. Data are taken from Ref. [17] ($N_f = 0$), Ref. [20] ($N_f = 2$) and Ref. [26] ($N_f = 3$). Dimensionless units are employed, with $\sqrt{\sigma} = 420$ MeV ($N_f = 0$ and $N_f = 2$) and $\sqrt{\sigma} = 460$ MeV ($N_f = 3$).

has to be fixed using some physical constraint. In Refs. [17, 20, 26] it has been normalized to match, at the shortest available distance for each temperature, the $T = 0$ heavy quark potential. Such a normalization amounts to make the (reasonable) assumption that thermal effects become negligible at very short distances.

In Refs. [17, 20] the zero temperature heavy quark potential has been determined through a best fit procedure of the available $T = 0$ lattice data with a Cornell-like parameterization³:

$$\frac{V(r)}{\sqrt{\sigma}} = -\frac{4}{3} \frac{\alpha}{r\sqrt{\sigma}} + \sqrt{\sigma}r, \quad (1)$$

σ representing the *string tension*. The values $\alpha = 0.195(1)$ for the case $N_f = 0$ and $\alpha = 0.212(3)$ for the case $N_f = 2$ are given in Ref. [20], where the value $\sqrt{\sigma} = 420$ MeV is employed to translate the lattice results into physical units.

In Ref. [26] a similar parameterization (Cornell potential plus a $1/r^2$ term to mimic the effects of asymptotic freedom at the shortest distances reachable on the lattice) is employed for the case $N_f = 3$. Note that in that work the free energy is provided directly in physical units: however, for the sake of comparison, we show it in dimensionless units, using for the string tension the value $\sqrt{\sigma} = 460$ MeV extracted from the parameterization of the $T = 0$ potential given in Ref. [26].

In past calculations [6, 7, 21, 22] the free energy has been often identified with the heavy quark potential and inserted directly into the Schrödinger equation. However, a better candidate for a more appropriate finite temperature potential is given by the internal energy of the $Q\bar{Q}$ system, defined by the well known relation

$$F = U - TS, \quad (2)$$

where

$$U = -T^2 \frac{\partial(F/T)}{\partial T} \quad (3)$$

is the internal energy and

$$S = -\frac{\partial F}{\partial T} \quad (4)$$

is the entropy. One can see from the data in Fig. 1 that the role played by the entropy is more relevant at large distances.

Getting the internal energy from the free energy involves a derivative of the latter with respect to the temperature: it is thus clear that one needs an accurate parameterization of the temperature dependence of F .

³ Note that the $1/r$ term accounts for two different physical processes: the perturbative one-gluon-exchange at short distances and the transverse string fluctuations at large distances.

In order to establish a suitable form for this parameterization of the lattice data, we first consider the two limits in which the underlying physics is supposed to be known.

At very short distances ($r \ll 1/T$) thermal effects are negligible and the colour singlet free energy is dominated by the perturbative one-gluon exchange with the typical behaviour:

$$F_1(r, T) \underset{rT \ll 1}{\sim} -\frac{4}{3} \frac{\alpha(r)}{r}, \quad (5)$$

the coupling α depending only upon the $Q\bar{Q}$ separation.

On the other hand, for $T \gg T_c$, the large distances ($r \gg 1/T$) behaviour of the free energy is expected to be dominated by the exchange of a resummed electrostatic gluon leading to the expression [27]:

$$F_1(r, T) \underset{rT \gg 1}{\sim} -\frac{4}{3} \frac{\alpha(T)}{r} e^{-m_D(T)r} + F_1(r = \infty, T). \quad (6)$$

In this limit, the coupling α is a function of the temperature and $m_D(T)$ is the Debye screening mass arising from the dressing of the electrostatic gluon.

In the two above limits, the running of the coupling is determined by a Renormalization Group Equation (RGE), allowing to express $\alpha = g^2/4\pi$ as a known (at least in the weak coupling regime) function of an energy scale μ . In the short distance limit the relevant energy scale is given by the inverse of the distance ($\mu \sim 1/r$), while for large separations the major role in setting the scale is expected to be played by the temperature ($\mu \sim T$).

Actually, in order to solve the Schrödinger equation for heavy quarkonia, one really needs a parameterization of the free energy covering the whole range of distances. For this purpose, on the basis of Eqs. (5) and (6) it appears convenient to cast the dependence of F_1 on r and T into the following functional form⁴:

$$F_1(r, T) = -\frac{4}{3} \frac{\alpha(r, T)}{r} e^{-M(T)r} + C(T). \quad (7)$$

In order to recover from the above the short and large distance limits given by Eqs. (5) and (6) one can, e.g., assume α to depend on the following combination of r and T :

$$\alpha(r, T) = \alpha(\mu = c_r/r + c_t T), \quad (8)$$

⁴ Note that the mass $M(T)$ appearing in this exponential will not necessarily coincide with the Debye screening mass of Eq. (6), the latter being determined by fitting only the large distance data.

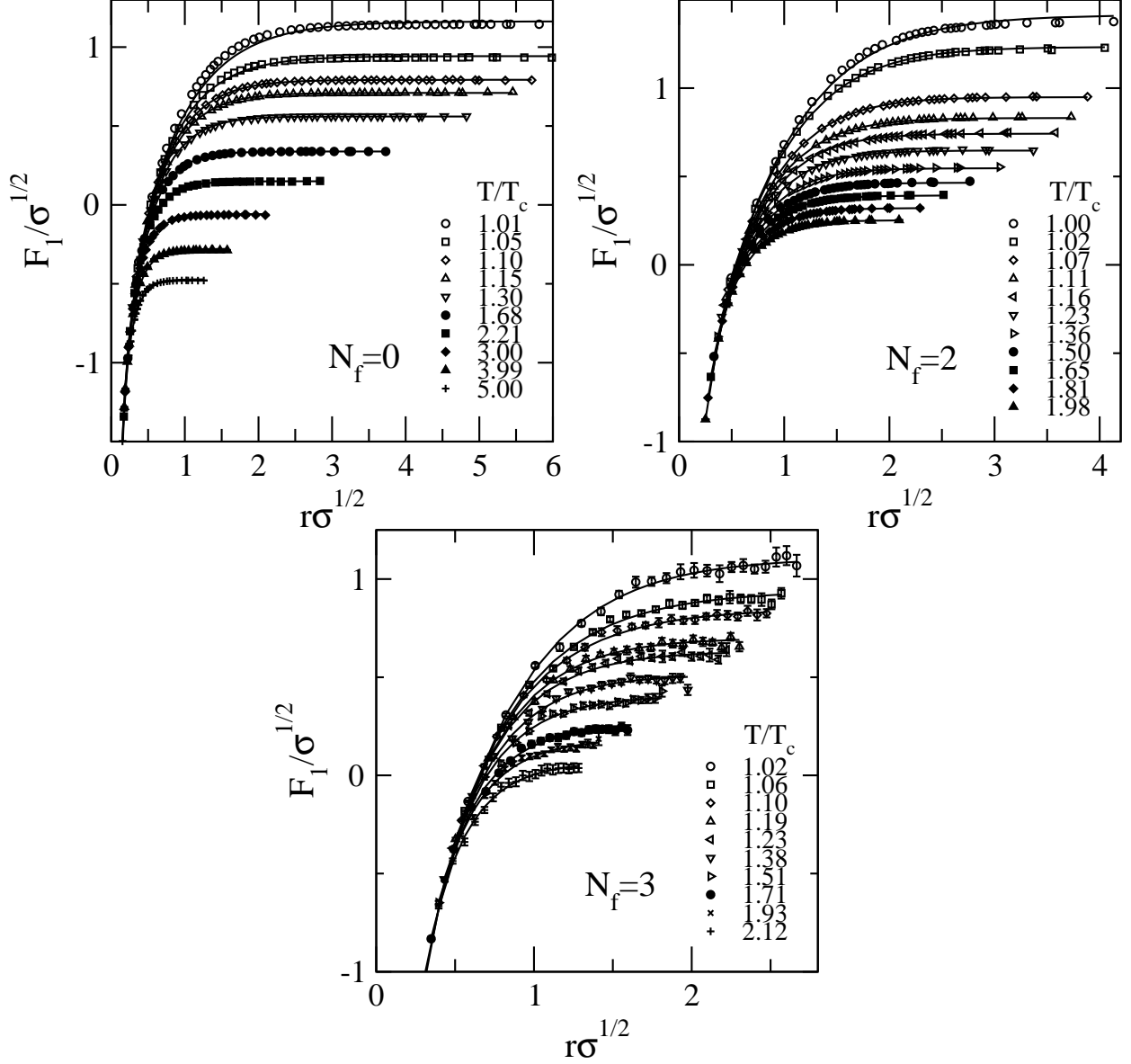


FIG. 2: The colour singlet free energy resulting from our fitting procedure compared to the lattice data at different temperatures above T_c .

where $\alpha(\mu)$ is obtained by solving the RGE, while c_r and c_t are numerical coefficients to be fixed through a best fit of the data.

If supported by the data, Eq. (8) would allow to interpolate between the short distance regime ($r \ll 1/T$), where $\mu \sim 1/r$, and the long distance one ($r \gg 1/T$), where on the contrary $\mu \sim T$.

We now describe in detail the fitting procedure we have employed. The data for the

colour singlet free energy, taken from Ref. [17] ($N_f = 0$), Ref. [20] ($N_f = 2$) and Ref. [26] ($N_f = 3$), are displayed in Fig. 1 in dimensionless units, namely $y = F_1/\sqrt{\sigma}$ and $x = r\sqrt{\sigma}$, for different values of the temperature both below and above T_c . For each value of $T > T_c$ the data have been parameterized with the following (four parameter) fitting function:

$$y = -\frac{4}{3} \frac{\alpha(\tilde{\mu})}{x} e^{-a_3 x} + a_0 \quad \text{with} \quad \tilde{\mu} = \frac{a_1}{x} + a_2 \quad (9)$$

where for $\alpha(\tilde{\mu})$ we use the RGE result obtained with the two-loop QCD beta-function quoted in Appendix A, the dimensionless variable $\tilde{\mu}$ being identified with the ratio μ/Λ_{QCD} .

The fitting procedure yields a very mild dependence on T for the parameters a_1 and a_2 . Actually, on the basis of the above discussion, one would have expected the coefficient a_2 to scale linearly with the temperature, but our finding might just signal that the range of temperatures spanned here is still not in the asymptotic regime $T \gg T_c$. On the other hand, a constant value for a_1 is in agreement with the ansatz of Eq. (8). This has suggested the following procedure: a weighted average of the values obtained for a_1 has been performed, yielding $a_1 = 0.2719(2)$ for $N_f = 0$, $a_1 = 0.2687(7)$ for $N_f = 2$ and $a_1 = 0.2354(17)$ for $N_f = 3$. We have then fitted again the data keeping a_1 fixed and using only a_0 , a_2 and a_3 as free parameters. This parameterization works well — yielding values of χ^2 per degree of freedom of the order of 1 at all the temperatures — and it is compared to the data in Fig. 2.

The finite temperature lattice data are limited to distances $r \gtrsim 0.1 \div 0.2$ fm. Since the data examined in this work have been normalized assuming that at short distances thermal effects are negligible, we should check that our parameterization does not introduce any sizable (and spurious) temperature dependence for small values of r , remaining in this region close to the $T = 0$ perturbative potential (we remind that at $T = 0$ free energy and internal energy coincide). In this respect our choice of refitting the data keeping the coefficient a_1 fixed fulfills this requirement.

The behaviour of our parameterization of the free energy for $r < 0.1$ fm is displayed, at three different temperatures, in Fig. 3 where we indeed see that spurious short distance thermal effects appears negligible. It is gratifying (and somewhat surprising) that our curves seems to interpolate smoothly between the $T = 0$ Cornell potential and the short distance perturbative potential. The Cornell curve reported in the figure is the one employed in Ref. [20] to fix the normalization of the free energy at the different temperatures. As already discussed at the beginning of this section it was obtained by fitting zero temperature

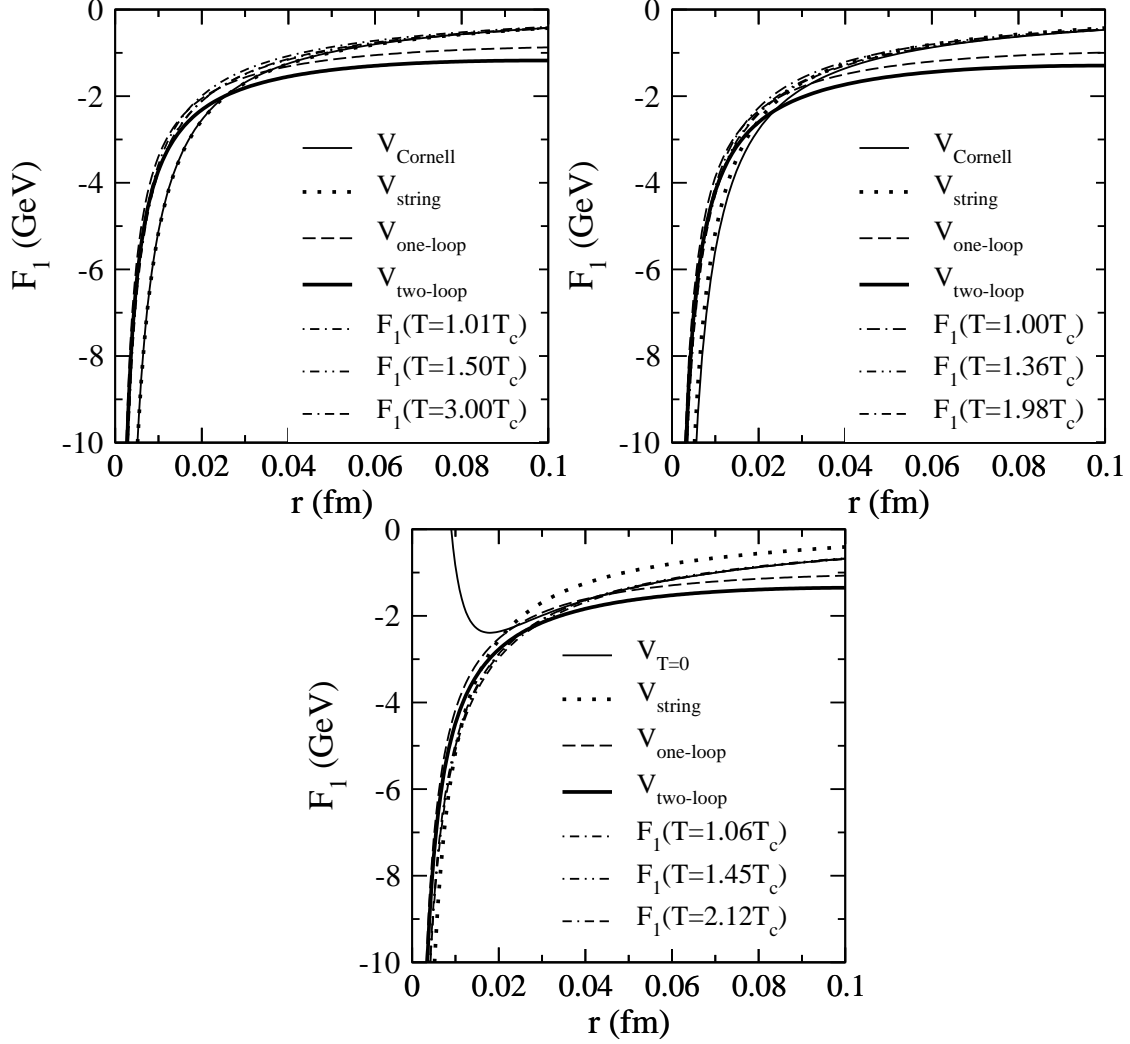


FIG. 3: The short distance behaviour of the colour singlet free energy resulting from our fits for different values of T/T_c . The dependence on the temperature turns out to be very small at such short distances. We also display for comparison the $T = 0$ potentials given by different schemes: the potentials employed to normalize the data at short distance [20, 26], the potential obtained in the Nambu string model and the one and two-loop short distance perturbative potentials [28, 29, 30].

lattice data which cover distances $r \gtrsim 0.05$ fm. Of course for shorter distances the Cornell parameterization cannot account for running coupling effects (asymptotic freedom) and the perturbative calculation [28, 29, 30] should provide more reliable results. More details on the one- and two-loop perturbative potential used in Fig. 3 are given in Appendix A.

The curves V_{string} reported in Fig. 3 refer to the $Q\bar{Q}$ potential

$$V(r) = -\frac{\pi}{12} \frac{1}{r} + \sigma r \quad (10)$$

obtained in the Nambu string model, the term $1/r$ arising from the quantum fluctuations of the flux tube in the transverse directions.

As a next step we have provided a parameterization of the T -dependence of a_0 , a_2 and a_3 , which allows one to perform analytically the derivative of F_1 with respect to the temperature (actually, for the calculation of the $Q\bar{Q}$ binding energies the knowledge of a_0 is unnecessary: we show also this contribution to the potential for completeness). Lacking compelling physical hints to the form of the T -dependence, we have sought for the simplest and smoothest expressions yielding a satisfactory interpolation of the values calculated from the fit to the lattice data (see Appendix B for details). The parameters and their interpolations are displayed in Fig. 4.

The value of $a_0(T)$ at each temperature is essentially fixed by the normalization of the data, which has been determined using similar procedures in all the lattice calculations. Notably this parameter, once plotted as a function of T/T_c , turns out to be fairly close for all values of N_f . On the other hand, the remaining two parameters display some quantitative flavor dependence, but within the same qualitative pattern. An exception to this behavior is represented by $a_2(T)$ for $N_f = 3$, although one should note that the three-flavor case is the one where the parameterization (9) has the largest uncertainties. Moreover, the variation of $a_2(T)$ with T is actually magnified by the scale of the figure, being generally around 20% for the range of temperatures considered here. As we shall see the resulting effective potential is rather robust with respect to these variations.

Note also that the strongest variation of the parameters with the temperature is confined around T very close to T_c . Since extracting the internal energy from F_1 involves a derivative with respect to T , this is the temperature domain where the sensitivity to the details of the parameterization might be high. For this reason we felt it safer to use the resulting potentials at temperatures larger than T_c , say for $T \gtrsim 1.05T_c$, where they turn out to be stable with respect to changes in the parameterization.

Finally, we recall that the quenched QCD data [17] are actually available also at temperatures much larger than those for the unquenched cases: here we limit our analysis up to about twice the critical temperature, since this is the range where lattice calculations with

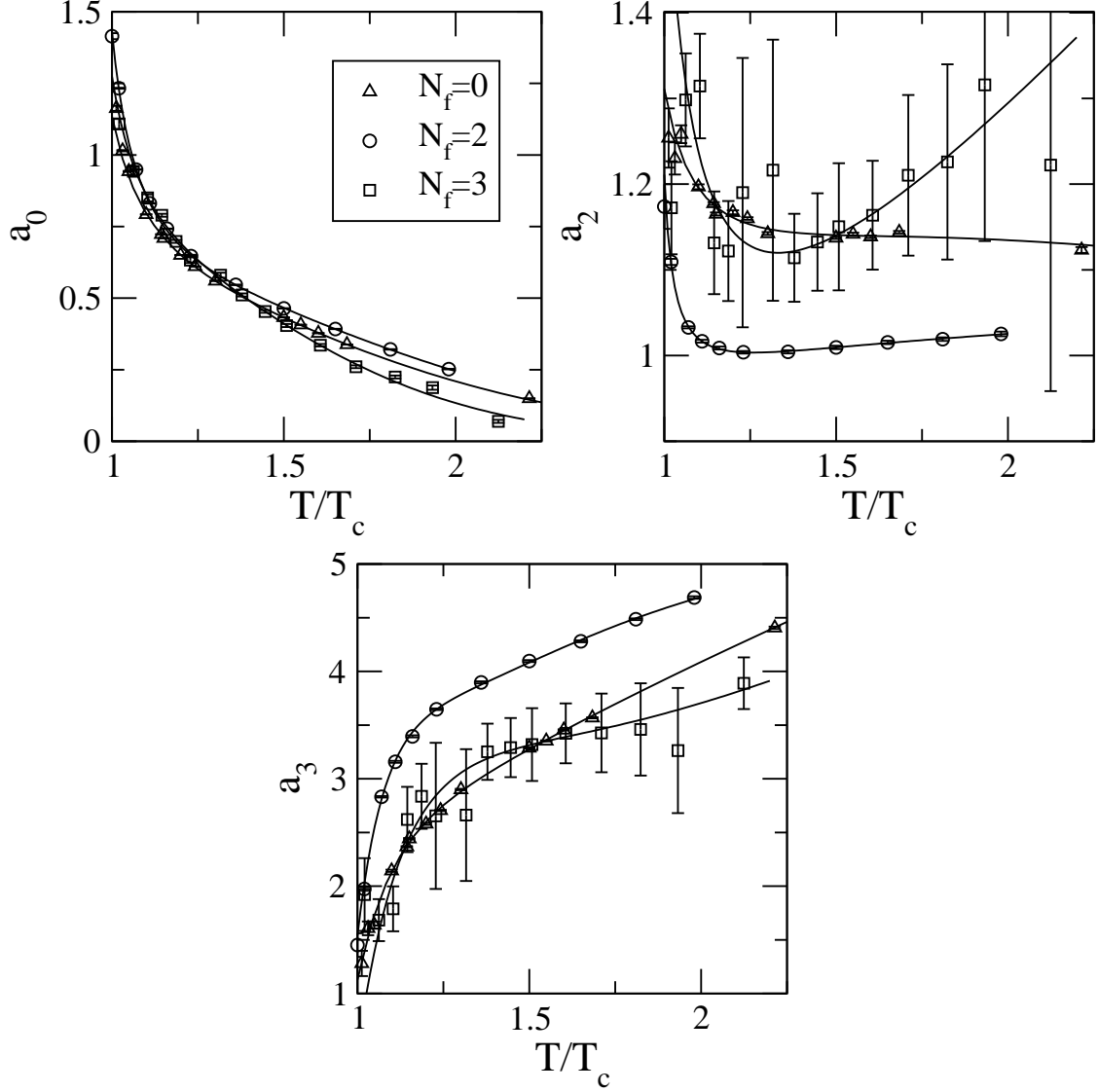


FIG. 4: Temperature dependence of the parameters a_0 , a_2 and a_3 employed in fitting the color singlet free energy with Eq. (9). The solid lines are interpolating functions.

two and three flavors are available and, moreover, since this is the range of interest for the problem of the J/ψ dissociation. Here we just remark that an analysis of the $N_f = 0$ data at larger temperatures (till $T \sim 5T_c$) with the parameterization of Eq. (9) shows that the fitting parameters maintain, also at these high temperatures, the trend displayed in Fig. 4.

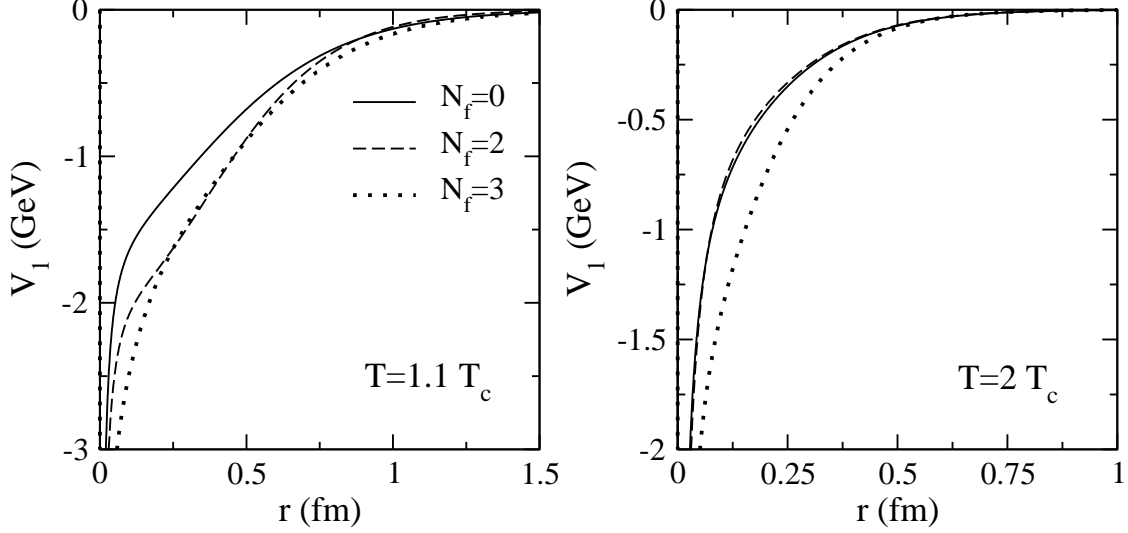


FIG. 5: The effective $Q\bar{Q}$ potentials extracted from the unquenched and quenched lattice calculations at two different temperatures.

III. $Q\bar{Q}$ BOUND STATES IN QUARK-GLUON PLASMA

The $Q\bar{Q}$ free energy obtained in lattice calculations has been used in the past as an input for the $Q\bar{Q}$ potential energy in the non-relativistic Schrödinger equation [6, 7, 21, 22]. More recently [17, 23, 24] it has been recognized that the $Q\bar{Q}$ potential energy can be more appropriately identified with the $Q\bar{Q}$ internal energy (see Eq. (3))⁵.

Once the temperature dependence of the color-singlet free energy F_1 has been parameterized, the corresponding color-singlet internal energy U_1 is easily obtained and one can define an effective potential

$$V_1(r, T) = U_1(r, T) - U_1(r \rightarrow \infty, T) \quad (11)$$

to be used in the Schrödinger equation

$$\left[-\frac{\nabla^2}{2\mu} + V_1(r, T) \right] \psi(\mathbf{r}, T) = \varepsilon(T) \psi(\mathbf{r}, T), \quad (12)$$

where μ is the reduced mass of the $Q\bar{Q}$ system.

⁵ Actually, the author of Ref. [23] tries to disentangle, in the total internal energy $U_1(r, T)$, the gluon and the $Q\bar{Q}$ contributions. This leads to a lower value for the J/ψ dissociation temperature with respect to the result $T_d \sim 2T_c$ obtained with the full internal energy.

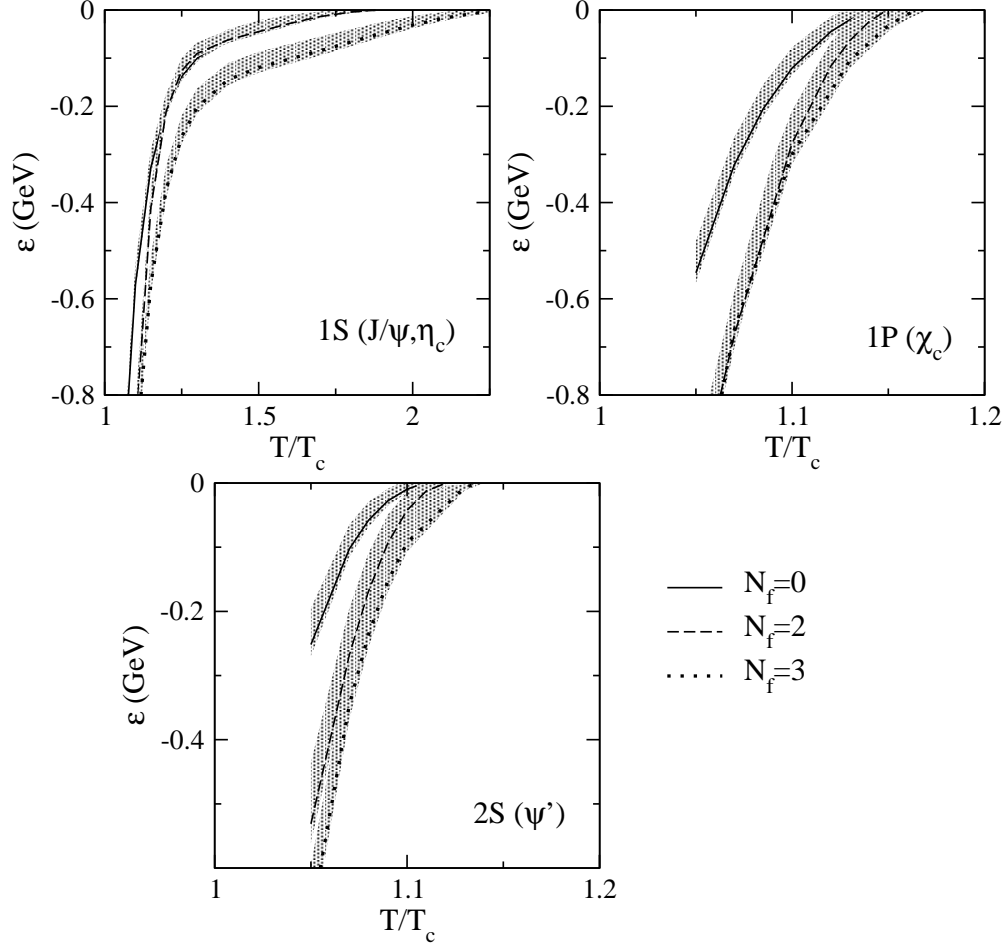


FIG. 6: Binding energy of charmonium states above the deconfinement temperature. The lines show the results for $m_c = 1.3$ GeV; the grey areas around the lines display the variations for $1.15 \text{ GeV} < m_c < 1.35 \text{ GeV}$.

In Fig. 5 we display, at two different temperatures, the effective $Q\bar{Q}$ potentials that we have obtained by using the parameterizations discussed in the previous section. At high temperature the form of V_1 is the one typical of a screened Coulomb potential, with the $N_f = 3$ potential providing a stronger attraction; at temperatures close to T_c the shape of V_1 appears somewhat distorted because of the strong temperature dependence of a_2 and a_3 (see Fig. 4), the $N_f = 3$ potential being still more attractive. Remarkably, the behaviour of the color singlet potential energies obtained with our procedure appears qualitatively in agreement with the one given in Refs. [18, 31], where the internal energy has been directly calculated on the lattice for $N_f = 0$ and $N_f = 2$, respectively.

We now employ the effective potential previously derived for the study of the charmonium and bottomonium spectroscopy above the critical temperature.

For what concerns the charmonium states we plot the values of the binding energies (Fig. 6) and of the mean square radii (Fig. 7) of the different bound state solutions of Eq. (12) as functions of T/T_c . For the sake of comparison the results obtained for a different number of dynamical fermions ($N_f = 0, 2, 3$) are plotted in the same panel.

In our analysis we have chosen $m_c = 1.3$ GeV for the charm quark mass; however, we have also studied the sensitivity of our results to variations of m_c in the range given in the Particle Data Group (PDG) listings [32], namely $1.15 \text{ GeV} < m_c < 1.35 \text{ GeV}$. For reference, in Fig. 7 the arrows point to the $T = 0$ mean square radii obtained in a potential model calculation [33]. Note that potential models at $T = 0$ typically follow a different philosophy: they fix the quark mass and the confining potential parameters to reproduce the mass of the lowest states, whereas here the potential is provided by lattice calculations and the quark mass is the running mass in the \overline{MS} scheme.

The $1P$ and $2S$ states turn out to melt at temperatures $1.1T_c \lesssim T_d \lesssim 1.15T_c$. On the contrary the J/ψ stays bound up to temperatures $1.7T_c \lesssim T_d \lesssim 2.3T_c$, the precise limits depending upon N_f . The lower bound ($T_d \sim 1.7T_c$) refers to the quenched case and appears in striking agreement with the limiting value obtained in Ref. [15] through the study of the J/ψ and η_c spectral functions.

Note that the free energy measured on the lattice provides a spin averaged result of the singlet and triplet channels: hence, in Figs. 6 and 7 the J/ψ and η_c mesons appear degenerate. This degeneracy is expected to be removed by a short range spin-spin force, whose effect, at $T = 0$, is often treated perturbatively assuming a contact interaction [34]:

$$H_{ss} = \frac{8\pi}{9} \frac{\alpha_s(\mu)}{m_q m_{\bar{q}}} \boldsymbol{\sigma}_q \cdot \boldsymbol{\sigma}_{\bar{q}} \delta(\mathbf{r}). \quad (13)$$

Again, the short range nature of this force makes plausible the assumption that it is not affected by thermal effects and that it can be employed also at finite temperatures. Then, for the J/ψ and η_c energy shifts one gets:

$$\Delta E_{J/\psi} = \frac{8\pi}{9} \frac{\alpha_s(\mu)}{m_c m_{\bar{c}}} |\psi(0, T)|^2 \quad (14a)$$

$$\Delta E_{\eta_c} = -\frac{24\pi}{9} \frac{\alpha_s(\mu)}{m_c m_{\bar{c}}} |\psi(0, T)|^2, \quad (14b)$$

where for $\alpha_s(\mu)$ we have used the two-loop expression of Eq. (A5), evaluated at $\mu = m_c$. As

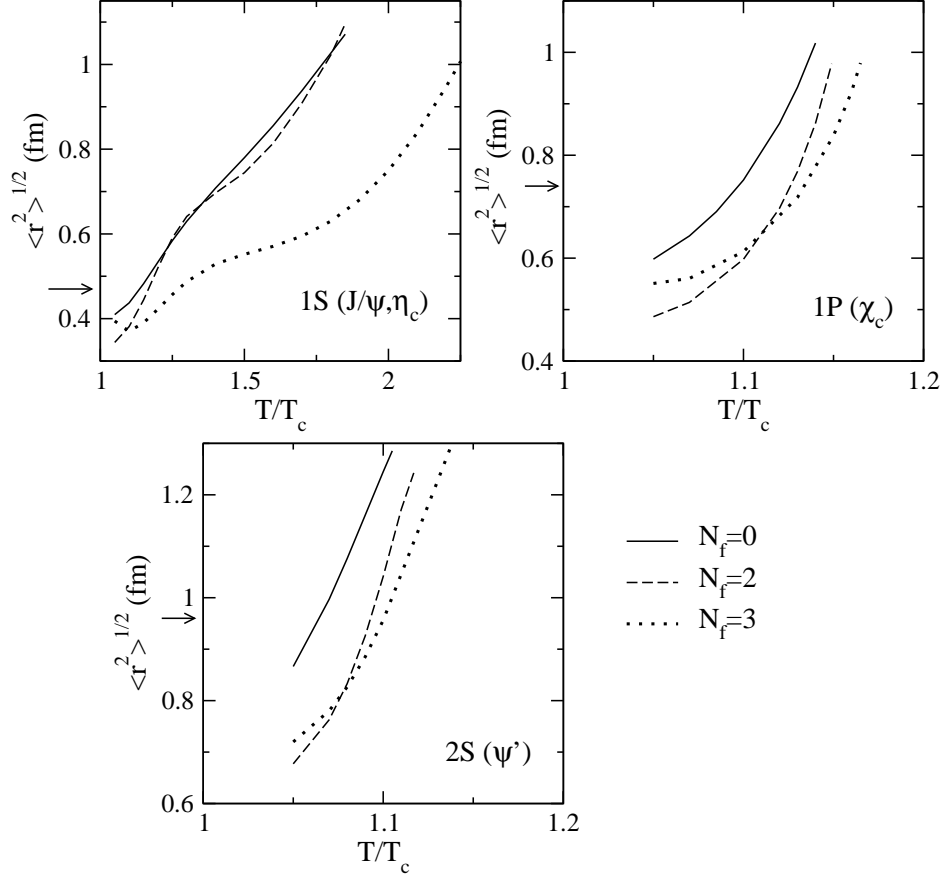


FIG. 7: Mean square radii of the charmonium states above the deconfinement temperature. The arrows point to the $T = 0$ results of Ref.[33]. The curves stop where the system is no longer bound.

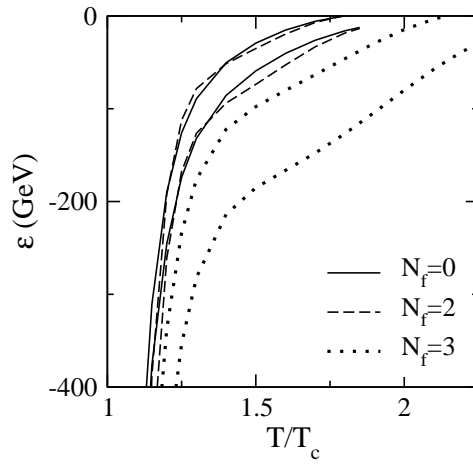


FIG. 8: Binding energy of the $1S, J = 1$ (J/ψ , upper lines) and $1S, J = 0$ (η_c , lower lines) states above the deconfinement temperature; $m_c = 1.3$ GeV.

one can see, the temperature dependance of this term stems entirely from the value of the $c\bar{c}$ wave function at the origin.

We display in Fig. 8 the binding energies of the J/ψ and η_c mesons above the deconfinement temperature. The spin-spin contribution gives rise to a mild reduction of the dissociation temperature, without altering the qualitative features of the results. For instance, for $N_f = 2$ at $T = 1.05T_c$ one gets a $J/\psi - \eta_c$ splitting of 145 MeV (the experimental value at $T = 0$ is about 117 MeV), whereas at the J/ψ melting temperature, $T \cong 1.8T_c$, one gets a splitting of 13 MeV (although, strictly speaking, in this case the perturbative expansion is no longer justified).

In Figs. 9 and 10 we plot the binding energies and the mean square radii of the bottomonium bound states above T_c . We have chosen $m_b = 4.3$ GeV for the bottom quark mass, but again we have studied the sensitivity to variations of m_b in the range of the PDG listings, $4.1 \text{ GeV} < m_b < 4.4 \text{ GeV}$. The arrows in Fig. 10 point to the results of $T = 0$ potential model calculations [33]. Of course, for heavier quark masses more states than in the charmonium case survive above the deconfinement temperature.

Both for the charmonium and for the bottomonium states the binding energy gets smaller and the mean square radius gets larger as the temperature grows. This should reflect into a huge increase of the elastic cross section $\sigma(Q\bar{Q} \rightarrow Q\bar{Q})$ at low energy. In fact, for a small relative momentum k of the two particles, when in the partial wave expansion the contribution of the s -wave is dominant, the presence of a $l = 0$ state near zero binding energy leads to a dramatic increase of the cross section as $k \rightarrow 0$, according to the formula:

$$\sigma_{l=0} \underset{k \rightarrow 0}{\sim} \frac{4\pi}{k^2 + 2\mu|\epsilon|}, \quad (15)$$

where μ is reduced mass of the system and ϵ the energy of the state near zero binding, no matter whether it is positive (virtual level) or negative (bound state). If something analogous happened also for the heavy-light states (for which lattice data are not available yet) this would clearly accelerate the thermalization of the heavy quarks.

From Figs. 5, 6 and 9 the effective potential obtained with $N_f = 3$ appears more attractive. Indeed the critical temperature T_c in the three cases $N_f = 0, 2, 3$ assumes different values, hence a naive comparison might not be so meaningful. Furthermore the finite temperature $N_f = 3$ lattice data available so far are affected by larger errors, so that our parameterization presents larger uncertainties with respect to the other two cases.

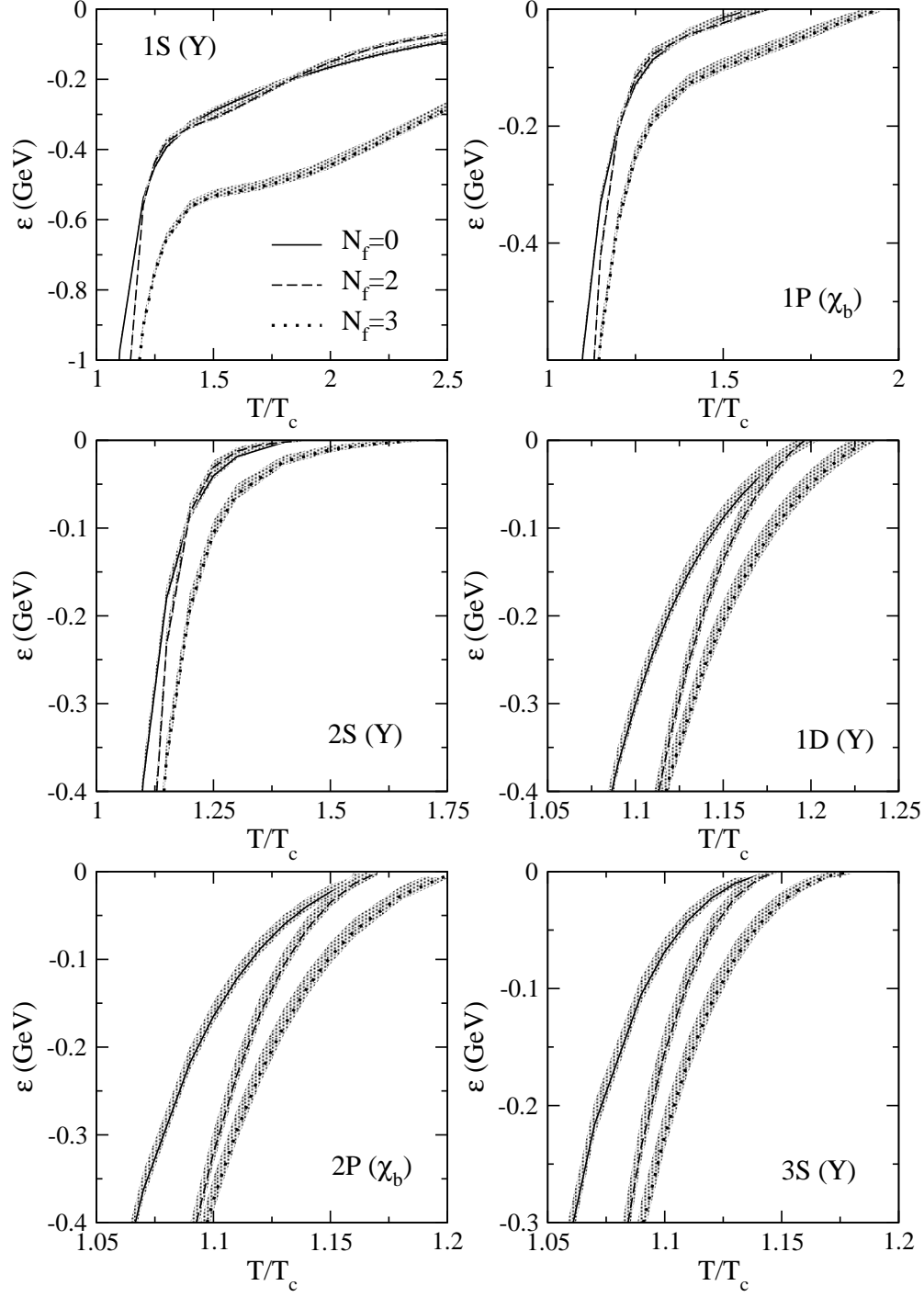


FIG. 9: Binding energy of the bottomonium states above the deconfinement temperature. The lines show the results for $m_b = 4.3 \text{ GeV}$; the grey areas around the lines display the variations for $4.1 \text{ GeV} < m_b < 4.4 \text{ GeV}$.

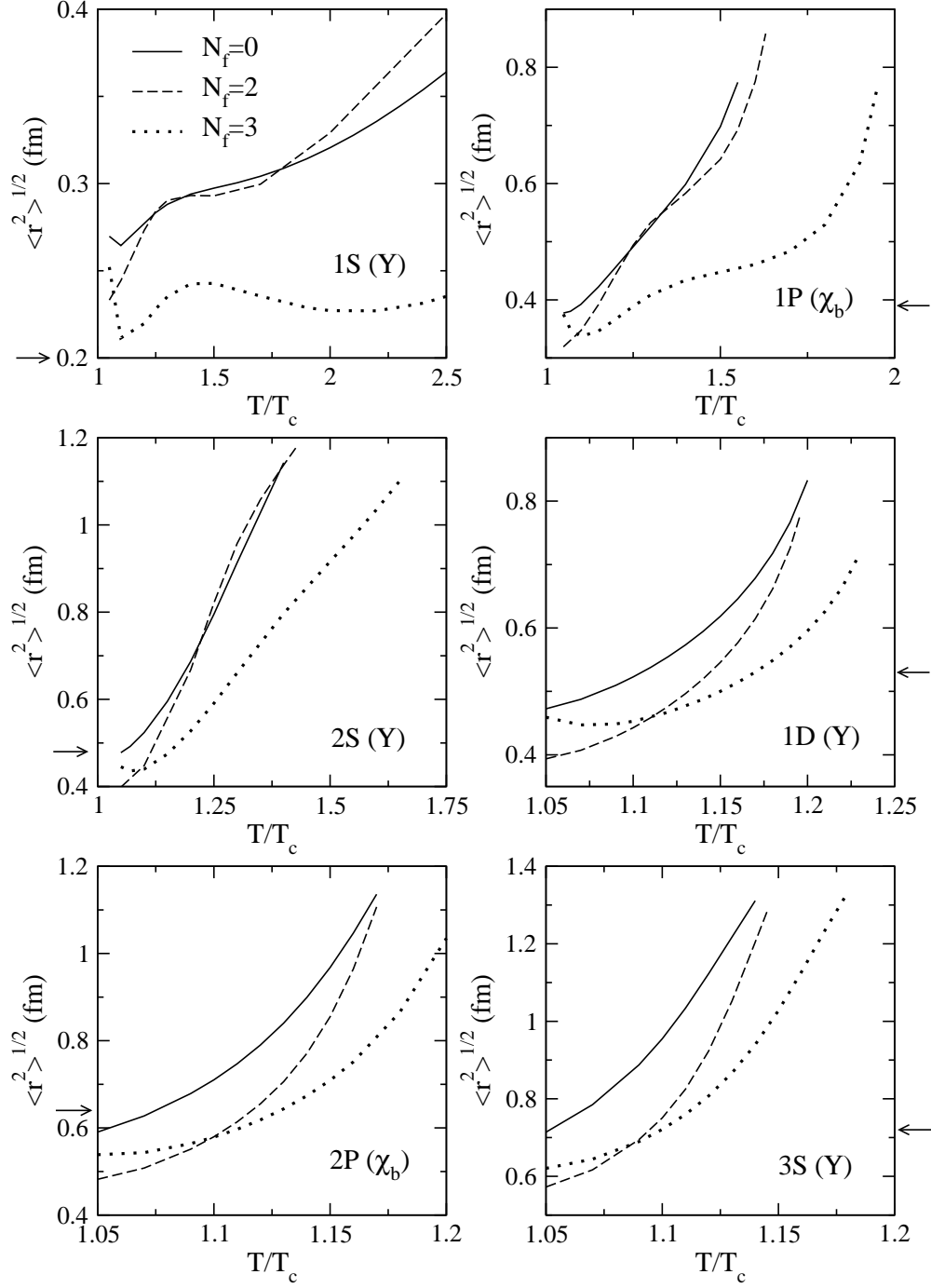


FIG. 10: Mean square radii of the bottomonium states above the deconfinement temperature. The arrows point to the $T = 0$ results of Ref.[33]. The curves stop where the system is no longer bound.

IV. CONCLUSIONS

The picture of the deconfined phase of QCD for values of the temperature slightly exceeding T_c — that is the ones accessible in the heavy-ion experiments presently performed at RHIC — has substantially evolved in the last few years.

For large values of the temperature ($T \gtrsim 3T_c$) a description of the QGP in terms of a gas of weakly interacting quasiparticles [35] appears reliable (even in a regime where the coupling g is not so weak) and supported by the lattice data for the QGP thermodynamics [36].

On the other hand, for temperatures up to $T \sim 2T_c$ (namely the ones currently accessible in the experiments), the matter resulting from the heavy-ion collisions is nowadays often described [24] as a strongly interacting QGP (sQGP). In particular, a striking feature of the QGP matter obtained at RHIC is its hydrodynamical behaviour [37, 38] (characterized by a very low viscosity), which manifests itself in particular in the elliptic flow [39] observed in non-central collisions: the plasma obtained at RHIC seems to behave as a nearly ideal fluid whose expansion is driven by pressure gradients.

In order to explain the very small mean free path of the plasma particles required by the hydrodynamical scenario, a picture of the matter obtained at RHIC in terms of a system of hundreds of loosely bound states of *quasiparticles* ($q\bar{q}$, qg , $gg\dots$) has been recently proposed [24]. In such a framework one has to resort to some assumptions. Gluons and light quarks are treated as quasiparticles endowed with quite heavy thermal masses obtained from lattice calculations and the potential felt by them in the different color channels is got from the lattice $Q\bar{Q}$ free energy under the hypothesis of *Casimir scaling*.

The presence of such a pattern of bound states in the range of temperatures $T_c \lesssim T \lesssim 2T_c$ has been recently questioned on the basis of the analysis of the correlation between baryon number and strangeness [40]. The evaluation of the correlation coefficient $C_{BS} = -3\langle BS \rangle / \langle S^2 \rangle$ should allow to discriminate between a scenario in which the relevant degrees of freedom in the QGP are weakly interacting quark and gluon *quasiparticles* or loosely bound states of the latters. The lattice data on the off-diagonal quark-number susceptibilities available so far seem to favour the first hypothesis.

Here we followed a different approach, starting from the case of a heavy $Q\bar{Q}$ pair placed in a thermalized QGP and extracting their interaction from the available lattice calculations.

Indeed, we have exploited the lattice data for the heavy quark free energies to get information on the existence of $c\bar{c}$ and $b\bar{b}$ bound states above the deconfinement transition. We have examined the cases $N_f = 0$ [17], $N_f = 2$ [20] and also $N_f = 3$ [26], where lattice data are getting available. For the color singlet free energy we have adopted a parameterization which accounts for the effects of asymptotic freedom at short distances and displays an exponential screening at large distances. From the free energy we have then extracted the heavy quark potential, to be inserted into the Schrödinger equation. The latter has been solved numerically for the two interesting cases of charmonium and bottomonium.

For what concerns the charmonium, we have found a dissociation temperature $T_d \sim 2T_c$ for the 1S states (η_c and J/ψ). Also the excited states 1P and 2S appear to melt, but at temperatures slightly exceeding T_c .

On the other hand, the bottomonium spectrum displays a much larger number of bound states above T_c . In particular its ground state turns out to remain bound in the whole range of temperatures covered by our parameterization. By extrapolating the latter at larger T we get a dissociation temperature $T_d \sim 4 \div 6T_c$, depending upon the number of dynamical fermions. At fixed T/T_c , both for the charmonium and for the bottomonium, the system turns out to be more bound when the number of light flavors is increased.

Remarkably, in the range of temperatures of experimental interest covered in this paper a number of loosely bound $Q\bar{Q}$ states exists. Since the existence of states near zero binding energy entails a huge increase of the elastic cross sections at low relative momenta, this can help the approach to thermal equilibrium also of the heavy quarks.

An analogous situation occurs in the cross-over from the BCS theory of superconductivity to the Bose-Einstein condensation, much explored lately in ensembles of alkaline fermionic atoms confined in a magnetic trap. Indeed, by smoothly changing the external magnetic field B , one induces a smooth change of the energy of the two interacting atoms: if this energy is close to the one of a Feshbach resonance, a huge increase in the cross-section occurs [41, 42, 43, 44]. The striking analogy between B and T as control parameters is self-imposing.

In connection with the previous discussion on heavy quark thermalization, it would be highly desirable to have lattice data also for the $Q\bar{q}$ states, which are not yet available.

A phenomenological model has been recently proposed assuming the existence of *resonant* (not bound) D- and B- meson states above T_c [45]. In this scheme the transverse

momentum distributions of the charmed quarks (anti-quarks) would approach their thermal equilibrium value much faster, due to isotropic resonant scattering on light anti-quarks (quarks). Indeed, recent PHENIX results for azimuthally averaged transverse momentum spectra of single electrons arising, in Au-Au collisions, from the decay of D- and B-mesons seem to be compatible with a thermalization scenario [46].

Furthermore, preliminary results from PHENIX and STAR on the elliptic flow of the above electrons tend to support a picture in which, due to strong rescattering, charmed quarks reach thermal equilibrium and follow the flow of the fireball [47, 48, 49, 50]. Hence, an extension of the present approach to the $Q\bar{q}$ ($q\bar{Q}$) states might shed light on the mechanism of thermalization of the heavy quarks.

Coming back to the present results, they offer the relevant possibility of evaluating the charmonium (bottomonium) multiplicity produced in heavy ion collisions at the experimental conditions of SPS, RHIC and LHC.

Indeed, a reliable estimate of the dissociation temperature of the different quarkonia is essential in order to predict how many of them, after being produced in the hard initial processes, survive in the QGP phase thus contributing to the final measured yields. The latter of course also contain, e. g., the charmonia that might be thermally produced during the hadronization process by $c\bar{c}$ recombination.

In particular, the knowledge of the in-medium quarkonium wave function and binding energy would allow a hopefully reliable estimate of the gluon-dissociation cross section of the J/ψ (and hence, via a detailed balance analysis, also of the cross section for the inverse process). Thus a kinetic rate equation accounting for both the dissociation and recombination processes can be tackled: its solution, depending on how many $c\bar{c}$ pairs are produced in the initial state, should provide the number of J/ψ present at the end of the QGP phase. These issues will be addressed in future work.

V. ACKNOWLEDGMENTS

We are grateful to O. Kaczmarek and P. Petreczky for providing us their lattice data. We wish to thank also C.Y. Wong for sending us a revised version of his paper.

APPENDIX A: RUNNING COUPLING AND PERTURBATIVE POTENTIALS AT SHORT DISTANCES

In this appendix we collect the formulas resulting from the perturbative calculations of Refs. [28, 29, 30] of the heavy quark potential at short distances, where asymptotic freedom guarantees that the perturbative approach is justified.

The static QCD potential turns out to be given by:

$$V(r) = -C_F \frac{\alpha_{\overline{MS}}(\mu)}{r} \left(1 + v_1(r, \mu) \frac{\alpha_{\overline{MS}}(\mu)}{\pi} + v_2(r, \mu) \frac{\alpha_{\overline{MS}}^2(\mu)}{\pi^2} + \dots \right), \quad (\text{A1})$$

where [29]

$$v_1(r, \mu) = \frac{1}{4} \left[\frac{31}{9} C_A - \frac{20}{9} T_F n_f + 2\beta_0 \log(\mu r') \right], \quad (\text{A2})$$

$$\begin{aligned} v_2(r, \mu) = & \frac{1}{16} \left[\left(\frac{4343}{162} + 4\pi - \frac{\pi^2}{4} + \frac{22}{3} \zeta_3 \right) C_A^2 - \left(\frac{1798}{81} + \frac{56}{3} \zeta_3 \right) C_A T_F n_f \right. \\ & - \left(\frac{55}{3} - 16\zeta_3 \right) C_F T_F n_f + \left(\frac{20}{9} T_F n_f \right)^2 + \beta_0^2 \left(4 \log^2(\mu r') + \frac{\pi^2}{3} \right) \\ & \left. + 2 \left(\beta_1 + 2\beta_0 \left(\frac{31}{9} C_A - \frac{20}{9} T_F n_f \right) \right) \log(\mu r') \right]. \end{aligned} \quad (\text{A3})$$

In the above $r' \equiv r \exp(\gamma_E)$ (γ_E is the Euler-Mascheroni constant), $C_A = 3$, $C_F = 4/3$, $T_F = 1/2$ and $\zeta_3 = \zeta_R(3)$ (the Riemann function of argument 3); moreover, $\alpha_{\overline{MS}}(\mu)$ is the QCD running coupling in the \overline{MS} renormalization scheme coming from the solution of the RGE:

$$\beta(\alpha_s(\mu^2)) = \frac{1}{\alpha_s(\mu^2)} \frac{\partial \alpha_s(\mu^2)}{\partial \log \mu^2} \equiv - \sum_{n=0}^{\infty} \beta_n \left(\frac{\alpha_s(\mu^2)}{4\pi} \right)^{n+1}. \quad (\text{A4})$$

The one-loop perturbative potential is by obtained keeping only the first two terms of Eq. (A1) and employing for $\alpha_{\overline{MS}}(\mu)$ the result

$$\alpha_{\overline{MS}}(\mu) = \frac{4\pi}{\beta_0 \ln \frac{\mu^2}{\Lambda_{\text{QCD}}^2}} \left(1 - \frac{\beta_1}{\beta_0^2} \frac{\ln \left(\ln \frac{\mu^2}{\Lambda_{\text{QCD}}^2} \right)}{\ln \frac{\mu^2}{\Lambda_{\text{QCD}}^2}} \right), \quad (\text{A5})$$

which arises from the solution of Eq. (A4) with the two-loop beta function (i.e. considering only the first two terms of the series). Indeed the coefficients β_0 and β_1 do not depend on the renormalization scheme and are given by:

$$\beta_0 = 11 - \frac{2}{3} N_f, \quad \beta_1 = 102 - \frac{38}{3} N_f. \quad (\text{A6})$$

On the other hand, for the two-loop perturbative potential one has to keep all the terms up to order α_s^3 displayed in Eq. (A1). The evaluation of the running coupling should include also the three-loop coefficient β_2 of the beta-function, which is no more renormalization scheme independent. In evaluating the two-loop curve in Fig. 3 we have used Eq. (13) of Ref. [51], where the \overline{MS} scheme is employed.

Clearly, Eq. (A1) still depends on the parameters μ and Λ_{QCD} . The scale $\mu \sim r^{-1}$ is quite arbitrary: we chose $\mu = [r \exp(\gamma_E)]^{-1}$ as usually done in the literature. For what concerns Λ_{QCD} we employed the value suggested by a recent lattice collaboration [51] $\Lambda_{\text{QCD}} = 261$ MeV for all the three cases ($N_f = 0, 2, 3$).

APPENDIX B: T -DEPENDENCE OF THE FIT PARAMETERS

In this appendix we show the functions employed in fitting the temperature dependence of the parameters $a_0(T)$, $a_2(T)$ and $a_3(T)$ entering into the functional form we have adopted for the $Q\bar{Q}$ free energy (see Sect. II).

As already mentioned in the text, since we have no phenomenological or theoretical hints to the functional form of the T -dependence of these parameters, we have tried to use the simplest expressions yielding a smooth fit and a “reasonable” χ^2 (say, of the order of a few units).

For $a_0(T)$ and $a_2(T)$ we have used the following forms:

$$a_0 = \frac{A_1^{(0)} x^{A_3^{(0)}} \exp[-A_0^{(0)} x]}{A_2^{(0)} x^2 - 1}, \quad (\text{B1})$$

$$a_2 = A_0^{(2)} \frac{A_1^{(2)} + A_2^{(2)} x^2 + x^4}{A_3^{(2)} + A_4^{(2)} x + x^3}, \quad (\text{B2})$$

where $x \equiv T/T_c$ and the $A_i^{(0)}$ ’s and $A_i^{(2)}$ ’s are fit parameters.

Only in the case of $a_3(T)$ we have used an expression inspired by perturbative QCD, namely the one for the Debye mass (although, rigorously this parameter does not represent the Debye mass):

$$a_3 = \left(1 + \frac{N_F}{6}\right)^{1/2} x \left(A_0^{(3)} + \frac{A_1^{(3)}}{x^2} + \frac{A_2^{(3)}}{x^4} + \frac{A_3^{(3)}}{x^6} + \frac{A_4^{(3)}}{x^8} \right) g_{2\text{-loop}}(x), \quad (\text{B3})$$

where $g_{2\text{-loop}}^2/4\pi \equiv \alpha_{\overline{MS}}$ is the 2-loop coupling constant obtained by replacing μ/Λ_{QCD} with $4.8826x \cong (2\pi T_c/\Lambda_{\text{QCD}})x$, having used $T_c = 202$ MeV and $\Lambda_{\text{QCD}} = 261$ MeV. In the case

$N_f = 3$, because of the larger errors affecting the parameterization of the free energy, we made the fit of a_3 stiffer by setting $A_4^{(3)} = 0$.

-
- [1] Abreu *et al.*, Phys. Lett. B **477**, 28 (2000).
 - [2] Na50 Collaboration, Eur. Phys. J. C **39**, 335 (2005).
 - [3] T. Matsui and H. Satz, Phys. Lett. B **178**, 416 (1986).
 - [4] R.L. Thews, hep-ph/0206179, in *New States of Matter in Hadronic Interactions*, edited by H.T. Elze, E. Ferreira, T. Kodama, J. Rafelski, and R.L. Thews (AIP, New York, 2002).
 - [5] S. Gupta and H. Satz, Phys. Lett. B **283**, 439 (1992).
 - [6] S. Digal, D. Petreczy, and H. Satz, Phys. Lett. B **514**, 57 (2001).
 - [7] S. Digal, D. Petreczy, and H. Satz, Phys. Rev. D **64**, 094015 (2001).
 - [8] F. Karsch, hep-lat/0502014.
 - [9] D. Kharzeev, C. Lourenco, M. Nardi, and H. Satz, Z. Phys. C **74**, 307 (1997).
 - [10] P. Braun-Munzinger and J. Stachel, Phys. Lett. B **490**, 196 (2000).
 - [11] L. Grandchamp and R. Rapp, Phys. Lett. B **523**, 60 (2001).
 - [12] L. Grandchamp and R. Rapp, Nucl. Phys. A **709**, 415 (2002).
 - [13] S. Datta, F. Karsch, P. Petreczy, and I. Wetzorke, Phys. Rev. D **69**, 094507 (2004).
 - [14] M. Asakawa, T. Hatsuda, and Y. Nakahara, Nucl. Phys. A **715**, 863 (2003).
 - [15] M. Asakawa and T. Hatsuda, Phys. Rev. Lett. **92**, 012001 (2004).
 - [16] L.D. McLerran and B. Svetitsky, Phys. Rev. D **24**, 450 (1981).
 - [17] O. Kaczmarek, F. Karsch, P. Petreczy, and F. Zantow, Phys. Lett. B **543**, 41 (2002).
 - [18] O. Kaczmarek, F. Karsch, P. Petreczy, and F. Zantow, Nucl. Phys. Proc. Suppl. **129**, 560 (2004).
 - [19] O. Kaczmarek, S. Ejiri, F. Karsch, P. Petreczy, and F. Zantow, Prog. Theor. Phys. Suppl. **153**, 287 (2004).
 - [20] O. Kaczmarek and F. Zantow, hep-lat/0503017.
 - [21] C.Y. Wong, Phys. Rev. C **65**, 034902 (2002).
 - [22] C.Y. Wong, J. Phys. G **28**, 2349 (2002).
 - [23] C.Y. Wong, hep-ph/0408020.
 - [24] E.V. Shuryak and I. Zahed, Phys. Rev. D **70**, 054507 (2004).

- [25] R.L. Thews, M. Schroedter, and J. Rafelski, Phys. Rev. C **63**, 054905 (2001).
- [26] P. Petreczky and K. Petrov, Phys. Rev. D **70**, 054503 (2004).
- [27] S. Nadkarni, Phys.Rev. D **33**, 3738 (1986).
- [28] M. Peter, Nucl.Phys. B **501**, 471 (1997).
- [29] M. Melles, Phys. Rev. D **62**, 074019 (2000).
- [30] Y. Schröder, Phys. Lett. B **447**, 321 (1999).
- [31] O. Kaczmarek and F. Zantow, hep-lat/0506019.
- [32] S. Eidelman et al. (Particle Data Group), Phys. Lett. B **592**, 1 (2004) (<http://pdg.lbl.gov>).
- [33] E. Eichten, K. Gottfried, T. Kinoshita, K. D. Lane, and T.M. Yan, Phys. Rev. D **21**, 203 (1980).
- [34] N. Brambilla *et al.*, hep-ph/0412158.
- [35] J.P. Blaizot, E. Iancu, and A. Rebhan, hep-ph/0303185, in *Quark Gluon Plasma 3*, edited by R.C. Hwa and X.N. Wang (World Scientific, Singapore, 2003), p. 60.
- [36] F. Karsch, E. Laermann, and A. Peikert, Phys. Lett. B **478**, 447 (2000).
- [37] D. Teaney, J. Laueret, and E. Shuryak, nucl-th/0110037.
- [38] P.F. Kolb and U.W. Heinz, nucl-th/0305084, in *Quark Gluon Plasma 3*, edited by R.C. Hwa and X.N. Wang (World Scientific, Singapore, 2003), p. 634.
- [39] J.Y. Ollitrault, Phys. Rev. D **46**, 229 (1992).
- [40] V. Koch, A. Majumder, and J. Randrup, nucl-th/0505052.
- [41] E. Timmermans, P. Tommasini, M. Hussein, and A. Kerman, Phys. Rep. **315**, 199 (1999).
- [42] A.J. Leggett, Rev. Mod. Phys. **73**, 307 (2001).
- [43] R.A. Duine and H.T.C. Stoof, Phys. Rep. **396**, 115 (2004).
- [44] K.M. O Hara, S.L. Hemmer, M.E. Gehm, S.R. Granade, and J.E. Thomas, Science **298**, 2179 (2002).
- [45] H. van Hees and R. Rapp, Phys. Rev. C **71**, 034907 (2005).
- [46] S. Batsouli, S. Kelly, M. Gyulassy, and J.L. Nagle, Phys. Lett. B **557**, 26 (2003).
- [47] PHENIX Collaboration (S. Kelly *et al.*), J. Phys. G **30**, S1189 (2004).
- [48] PHENIX Collaboration (S.S. Adlet *et al.*), nucl-ex/0502009.
- [49] STAR Collaboration (F. Laue *et al.*), J. Phys. G **G31**, S27 (2005).
- [50] V. Greco, C.M. Ko, and R. Rapp, Phys. Lett. B **595**, 202 (2004).
- [51] M. Gockeler *et al.*, hep-ph/0502212.